4

Time-Domain Analysis of Linear Control Systems

4.1 LINEARIZED RESPIRATORY MECHANICS: OPEN-LOOP VERSUS CLOSED-LOOP

In the previous chapter, we considered how feedback can change the steady-state behavior of physiological systems. In this chapter, we will explore the basic concepts and analytical techniques used to quantify the dynamics of *linearized* physiological models. We will perform extensive mathematical analyses of models with first-order and second-order dynamics. These are models that one can employ as "first approximations" to a number of physiological systems. They are useful in demonstrating the methods of analysis and concepts that can be applied, while allowing the mathematics to remain at a manageable, nondistracting level.

We consider a simplified version of the linearized lung mechanics model discussed in Section 2.3. Instead of the several regional resistances and compliances, this model contains only one resistance (R) and one compliance (C) element which represent, respectively, the overall mechanical resistive and storage properties of the respiratory system. Thus, R represents a combination of resistance to airflow in the airways, lung tissue resistance, and chest-wall resistance. C represents the combined compliance of lung tissue, chest wall, and airways. In addition, however, we will also add an inductance element, L, that represents fluid inertance in the airways. The electrical analog of this model is displayed in Figure 4.1. Our task is to predict how the alveolar pressure, P_A, will respond dynamically to different pressure waveforms (P_{ao}) applied at the airway opening.

Applying Kirchhoff's First Law (see Section 2.2) to the model, we find that the pressure drop across the entire model must be equal to the sum of all the pressure drops across each of the circuit elements. Thus,

$$P_{ao} - P_0 = L\frac{dQ}{dt} + RQ + \frac{1}{C}\int Q\,dt \tag{4.1}$$

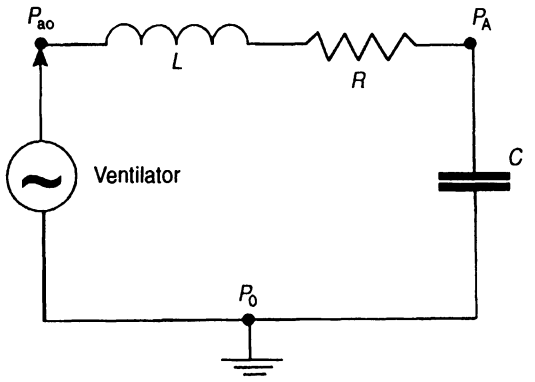

Figure 4.1 Electrical analog of lung mechanics model.

In Equation (2.9), Q represents the airflow rate. A similar expression can be derived to relate P_A to Q:

$$P_A - P_0 = \frac{1}{C}\int Q\,dt \tag{4.2}$$

We will reference all pressures to the ambient pressure (i.e., set $P_0 = 0$). Combining Equations (4.1) and (4.2), and eliminating Q from both equations, we obtain

$$P_{ao} = LC\frac{d^2P_A}{dt^2} + RC\frac{dP_A}{dt} + P_A \tag{4.3}$$

Equation (4.3) describes the dynamic relationship between P_{ao} and P_A. Applying the Laplace transform to this second-order differential equation yields the transfer function of the model:

$$\frac{P_A(s)}{P_{ao}(s)} = \frac{1}{LCs^2 + RCs + 1} \tag{4.4}$$

This transfer function is displayed schematically in Figure 4.2a. Note that, since P_A is entirely dependent on P_{ao}, this depicts an *open-loop* configuration.

Let us now consider an alternative situation where we would like to be able to attenuate the changes in P_A as much as possible, for a given set of lung mechanical parameters and a given imposed change in P_{ao}. In the clinical setting, this is desirable, since large fluctuations

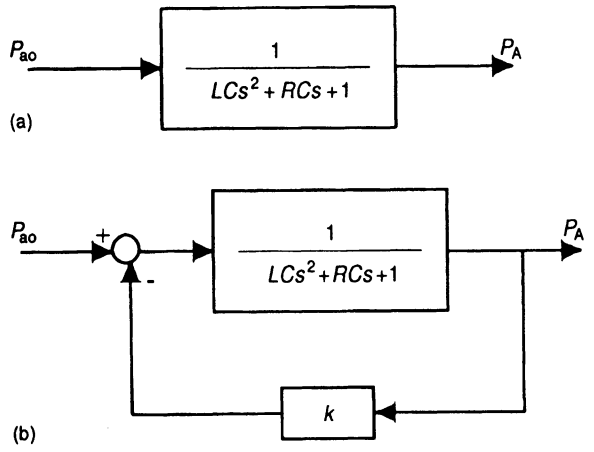

Figure 4.2 (a) Lung mechanics model—open-loop configuration. (b) Lung mechanics model—closed-loop configuration.

in P_A can cause pulmonary barotrauma or damage to lung tissue. In order to "control" P_A, it is necessary to measure this variable and feed the measurement back to the controller. In practice, this can be achieved by measuring the pressure in the mid-esophagus with the use of an esophageal balloon, since fluctuations in esophageal pressure have been demonstrated to closely reflect fluctuations in alveolar pressure. Thus, we assume the arrangement shown in Figure 4.2b, where P_A is measured and a scaled representation of this measurement is fed back and subtracted from the input, P_{ao}. This clearly is a *closed-loop* configuration and the type of control scheme is known as *proportional feedback*, since the feedback variable is proportional to the system output. Reanalysis of the new block diagram yields the following result:

$$\frac{P_A(s)}{P_{ao}(s) - kP_A(s)} = \frac{1}{LCs^2 + RCs + 1} \tag{4.5a}$$

By rearranging terms in Equation (4.5a), we can derive the following expression for the overall transfer function of the closed-loop system:

$$\frac{P_A(s)}{P_{ao}(s)} = \frac{1}{LCs^2 + RCs + (1 + k)} \tag{4.5b}$$

Equations (4.4) and (4.5b) can be generalized to represent both the open-loop and closed-loop conditions:

$$\frac{P_A(s)}{P_{ao}(s)} = \frac{1}{LCs^2 + RCs + \lambda} \tag{4.6}$$

where $\lambda = 1$ for the open-loop case, and $\lambda = 1 + k$ for the closed-loop case.

4.2 OPEN-LOOP AND CLOSED-LOOP TRANSIENT RESPONSES: FIRST-ORDER MODEL

In the range of spontaneous breathing frequencies, studies with reasonably realistic models of respiratory mechanics, such as that by Jackson and Milhorn (1973), have demonstrated that airway fluid inertance plays a virtually insignificant role in determining lung pressures and airflow. Thus, under these conditions, we can ignore inertance effects by setting L to zero. The transfer function in Equation (4.6) then becomes

$$\frac{P_A(s)}{P_{ao}(s)} = \frac{1}{\tau s + \lambda} \tag{4.7}$$

where $\tau = RC$.

4.2.1 Impulse Response

We can obtain the impulse response, $h_1(t)$, of the first-order system in Equation (4.7) by setting $P_{ao}(s)$ to 1, since we are assuming the input to take the form of a unit impulse. We also multiply both numerator and denominator of the right-hand side of Equation (4.7) by $1/\tau$ to reduce it to the standard form:

$$P_A(s) = \frac{1/\tau}{s + \lambda/\tau} \tag{4.8}$$

Using the table of Laplace transforms in Appendix I, it can be seen that the impulse response is

$$h_1(t) = \frac{1}{\tau} e^{-(\lambda/\tau)t} \tag{4.9}$$

Thus, the impulse response under both open-loop and closed-loop conditions is a simple exponential. Note that the peak of the impulse response is a function only of τ, which depends on the system parameters R and C, but not of λ, i.e., it is the same value under open-loop and closed-loop conditions. However, the time constant of the exponential is τ/λ. Without proportional feedback, this time constant is τ, since λ is unity. However, with proportional feedback, $\lambda > 1$; therefore, the closed-loop impulse response decays faster. Theoretically, the "response time" of the system can be made infinitely fast if the feedback gain, k, is raised to an infinitely high level. A comparison of open-loop and closed-loop responses is shown in Figure 4.3a for the case where $R = 1\ \text{cm}\,H_2O\,\text{s}\,L^{-1}$, $C = 0.1\ \text{L}\,\text{cm}\,H_2O^{-1}$, and $\lambda = 2$ (i.e., $k = 1$).

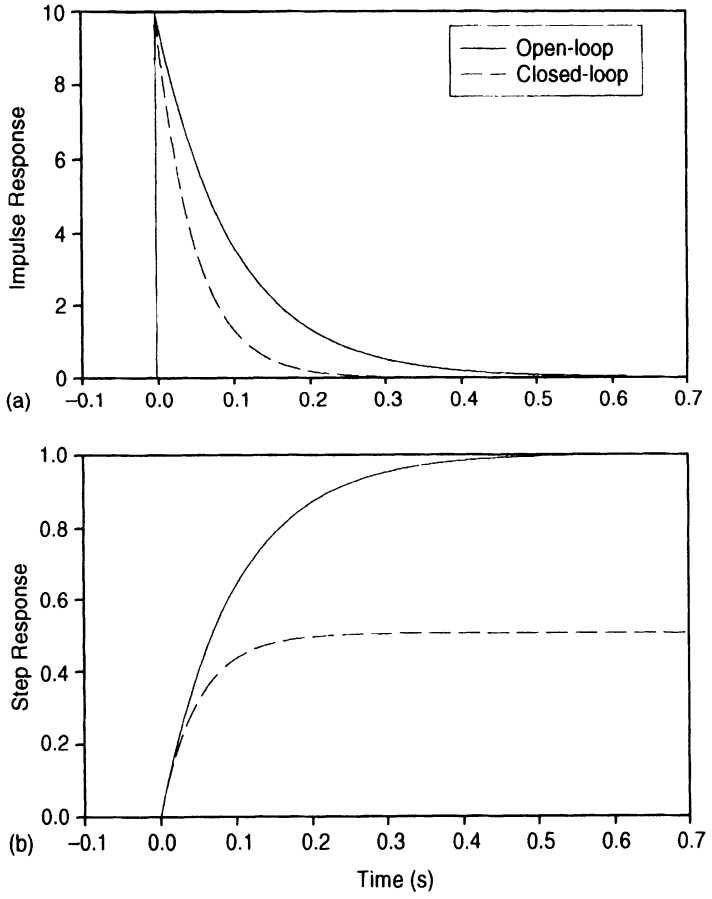

Figure 4.3 (a) Response of first-order lung mechanics model to a unit impulse. (b) Response of first-order lung mechanics model to a unit step. Solid and dashed lines represent the model responses in open-loop and closed-loop modes. Parameter values used: $R = 1\ \text{cm}\,H_2O\,\text{s}\,L^{-1}$, $C = 0.1\ \text{L}\,\text{cm}\,H_2O^{-1}$, $\lambda = 2$.

4.2.2 Step Response

To deduce the response, $g_1(t)$, of the first-order model to a unit step, we set $P_{ao}(s)$ to $1/s$ and rearrange Equation (4.7) to obtain

$$P_A(s) = \frac{1/\tau}{s(s + \lambda/\tau)} \tag{4.10}$$

Again, the corresponding response in the time-domain can be found by using Appendix I:

$$g_1(t) = \frac{1}{\lambda}\left(1 - e^{-(\lambda/\tau)t}\right) \tag{4.11}$$

As in the case for the impulse response, the time constant for the step response is decreased when proportional feedback is introduced, i.e., the closed-loop system responds faster. Whereas the peak amplitude of the impulse response is not affected by feedback, the steady-state magnitude of the closed-loop step response is inversely proportional to λ. Thus, the greater the feedback gain, k, the smaller the steady-state value of the closed-loop step response. This can also be expressed as the *steady-state error*, ε_1, defined as the final ($t \to \infty$) difference between the input (which is the unit step function) and the closed-loop step response. Thus, in this case, ε_1 increases as k and λ increase:

$$\varepsilon_1|_{t\to\infty} = 1 - \frac{1}{\lambda} \tag{4.12}$$

Figure 4.3b compares the step responses of the first-order open-loop and closed-loop respiratory mechanics model for the same parameter values as in Figure 4.3a. In the open-loop case, there is no steady-state error.

4.3 OPEN-LOOP VERSUS CLOSED-LOOP TRANSIENT RESPONSES: SECOND-ORDER MODEL

We now turn to the more general situation, which covers a larger range of respiratory frequencies. As the rates of change of airflow become larger, so will the effects derived from fluid inertance, L. This brings us back to the second-order model represented by Equation (4.6).

4.3.1 Impulse Responses

To deduce the impulse response, $h_2(t)$, of the second-order system, we set $P_{ao}(s) = 1$ in Equation (4.6), which becomes

$$P_A(s) = \frac{1/LC}{s^2 + (R/L)s + \lambda/LC} \tag{4.13}$$

To determine the inverse Laplace transform of Equation (4.13), it is necessary to evaluate the roots of the quadratic function in s. If we denote the roots by α_1 and α_2, then

$$\alpha_{1,2} = -\frac{R}{2L} \pm \sqrt{\frac{R^2}{4L^2} - \frac{\lambda}{LC}} \tag{4.14}$$

Depending on the values of the model parameters, the roots α_1 and α_2 can be imaginary, complex, real and equal, or real and different. As we will demonstrate below, these roots

determine whether the model behavior is oscillatory, underdamped, critically damped, or overdamped. We will consider each of these cases individually.

4.3.1.1. Undamped Behavior. The roots α_1 and α_2 are imaginary when $R = 0$, so that Equation (4.13) becomes

$$P_A(s) = \frac{1/LC}{s^2 + \lambda/LC} \tag{4.15}$$

Thus, the roots are

$$\alpha_1 = j\sqrt{\frac{\lambda}{LC}} \quad \text{and} \quad \alpha_2 = -j\sqrt{\frac{\lambda}{LC}} \tag{4.16a,b}$$

The inverse Laplace transform of Equation (4.15) is

$$h_2(t) = \frac{1}{\sqrt{\lambda LC}} \sin\left(\sqrt{\frac{\lambda}{LC}}\, t\right) \tag{4.17}$$

Equation (4.17) implies that the response of the model to an impulsive change in P_{ao} is a sustained oscillation. In the *open-loop* configuration ($\lambda = 1$), the amplitude and the angular frequency of this oscillation are equal in magnitude, with both assuming values of $(LC)^{-1/2}$. However, in the *closed-loop* situation, $\lambda > 1$, which lowers the amplitude of the oscillation but increases its frequency. These responses are shown graphically in Figure 4.4a. In the example displayed, we have assumed the following parameter values: $L = 0.01\ \text{cm}\,H_2O\,s^2\,L^{-1}$ and $C = 0.1\ \text{L cm}\,H_2O^{-1}$. Under open-loop conditions, these parameter values produce an oscillation of frequency $(1000)^{1/2}/(2\pi)$ Hz, or approximately, 5 Hz. As in Section 4.2.1, we again assume the feedback gain, k, is set equal to unity, so that $\lambda = 2$. Then, the closed-loop oscillation amplitude will be $1/\sqrt{2}$ times, or approximately 71%, the oscillation amplitude in the open-loop case. At the same time, the oscillation frequency will be $\sqrt{2}$ times the corresponding value under open-loop conditions, or approximately 7 Hz.

4.3.1.2. Underdamped Behavior. The sustained oscillatory responses in the previous section are, of course, highly unrealistic, since they require that R be reduced to zero. Consider now the situation when R is nonzero but small, so that

$$\frac{R^2}{4L^2} < \frac{\lambda}{LC} \tag{4.18}$$

The term within the square-root operation in Equation (4.14) will become negative, and consequently, the characteristic roots α_1 and α_2 will be complex. Equation (4.13) then becomes

$$P_A(s) = \frac{1/LC}{\left(s + \frac{R}{2L}\right)^2 + \left(\frac{\lambda}{LC} - \frac{R^2}{4L^2}\right)} \tag{4.19}$$

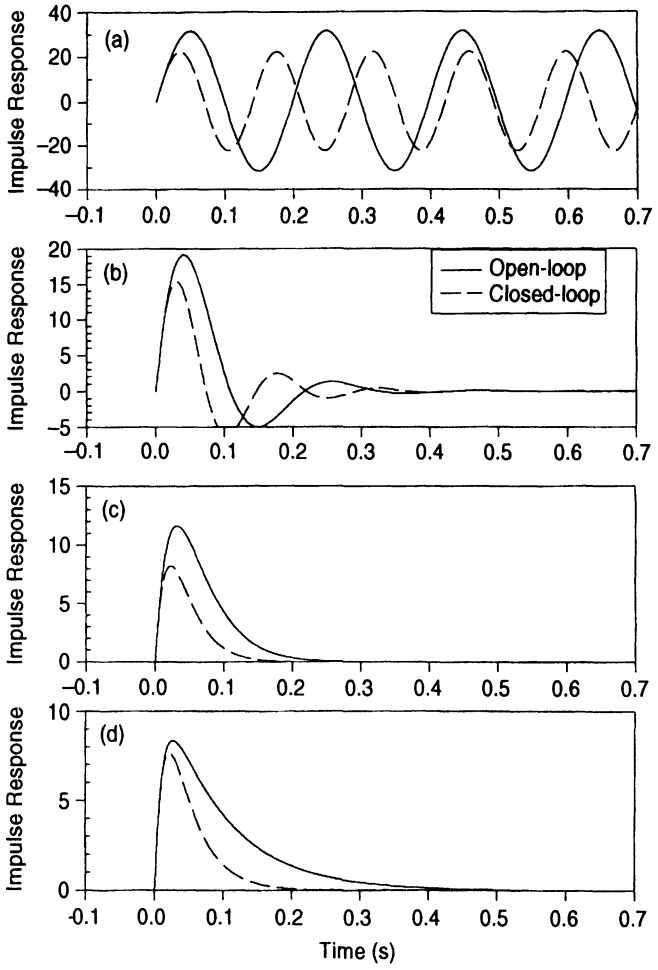

Figure 4.4 Responses of the second-order lung mechanics model to a unit impulse under open-loop (solid lines) and closed-loop (dashed lines) modes: (a) undamped responses; (b) underdamped responses; (c) critically damped responses; and (d) overdamped responses.

which is easily converted to the standard form

$$P_A(s) = \frac{1/LC}{\left(s + \frac{R}{2L}\right)^2 + \gamma^2} \tag{4.20}$$

where

$$\gamma = \frac{R}{2L}\sqrt{\left(\frac{4L\lambda}{R^2C} - 1\right)} > \frac{R}{2L} \tag{4.21}$$

From Equation (4.14), the characteristic roots of the denominator are clearly

$$\alpha_{1,2} = -\frac{R}{2L} \pm j\gamma \tag{4.22}$$

Applying the inverse Laplace transform to Equation (4.20), we obtain the following impulse response:

$$h_2(t) = \frac{1}{LC\gamma} e^{-(R/2L)t} \sin(\gamma t) \tag{4.23}$$

The above result shows that, in the underdamped situation, the model responds to a unit impulse with dynamics that can be described as a damped sinusoid. Note that, in the limit when R decreases to zero, Equation (4.23) degenerates into the sustained oscillation represented by Equation (4.17).

How does the incorporation of negative feedback affect this underdamped response? In the closed-loop situation, λ becomes larger than unity, which increases γ relative to the open-loop case. This, in turn, reduces the amplitude of the damped oscillations but increases their frequency. However, the exponential decay term is unaffected by λ. A graphical comparison of underdamped impulse responses under open-loop versus closed-loop conditions is displayed in Figure 4.4b. In this example, the values of L and C are the same as those employed in Section 4.3.1.1. The value of R used here is 0.5 (cm H_2O) s L^{-1}. With these parameter values, $\gamma = 19.4$ in the open-loop case; thus, the frequency of the damped oscillation is approximately 3 Hz. With the incorporation of negative feedback ($k = 1$, so that $\lambda = 2$), $\gamma \approx 37.1$ so that the damped oscillation frequency becomes approximately 6 Hz. At the same time, the amplitude of the damped oscillation in the closed-loop case is significantly lower than that in the open-loop case.

4.3.1.3. Critically Damped Behavior. If R is increased further until the following condition becomes valid:

$$\frac{R^2}{4L^2} = \frac{\lambda}{LC} \tag{4.24}$$

γ will become zero and Equation (4.13) will reduce to

$$P_A(s) = \frac{1/LC}{\left(s + \frac{R}{2L}\right)^2} \tag{4.25}$$

Thus, in this case, the characteristic roots will be real and equal, as shown below:

$$\alpha_{1,2} = -\frac{R}{2L} \tag{4.26}$$

The inverse Laplace transform of Equation (4.25) yields the impulse response of the model:

$$P_A(t) = \frac{1}{LC} te^{-t/\tau_c} \tag{4.27}$$

where

$$\tau_c = \frac{2L}{R} = \sqrt{\frac{LC}{\lambda}} \tag{4.28}$$

Note that the second part of Equation (4.28) follows directly from the equality condition expressed in Equation (4.24).

The above results demonstrate that, in the critically-damped mode, all oscillatory behavior disappears. How is the response affected by the introduction of negative feedback?

Equation (4.28) shows quite clearly that, in the closed-loop configuration where $\lambda > 1$, the single time constant for the exponential decay is shorter compared to the open-loop case when $\lambda = 1$. Thus, as was the case for the first-order model, proportional feedback increased the speed of response of the system. This comparison is displayed graphically in Figure 4.4c. However, compared to the open-loop case, we see from Equation (4.24) that R has to be increased to a higher value before the damped oscillatory behavior disappears and critical damping is achieved in the closed-loop system.

4.3.1.4. Overdamped Behavior. When R increases above the point at which critical damping occurs, the following inequality will take effect:

$$\frac{R^2}{4L^2} > \frac{\lambda}{LC} \tag{4.29}$$

Under these circumstances, the characteristic roots of Equation (4.14) become real and different:

$$\alpha_1, \alpha_2 = -\frac{R}{2L}(1 \pm \mu) \tag{4.30}$$

where

$$\mu = \sqrt{1 - \frac{4L\lambda}{R^2C}} \tag{4.31}$$

It follows from the inequality expressed in Equation (4.29) that μ must lie between zero and unity in Equation (4.31). The resulting expression for $P_A(s)$ becomes

$$P_A(s) = \frac{\dfrac{1}{LC}}{\left(s + \dfrac{R}{2L}(1-\mu)\right)\left(s + \dfrac{R}{2L}(1+\mu)\right)} \tag{4.32}$$

Consequently, the inverse transform of Equation (4.32) yields

$$h_2(t) = \frac{1}{\mu RC}(e^{-t/\tau_1} - e^{-t/\tau_2}) \tag{4.33}$$

where

$$\tau_1 = \frac{2L}{R(1-\mu)} \quad \text{and} \quad \tau_2 = \frac{2L}{R(1+\mu)} \tag{4.34a,b}$$

Thus, in the overdamped system, the impulse response is composed of two exponential decay contributions with larger time constant τ_1 and smaller time constant τ_2.

To compare the overdamped impulse responses in the closed-loop versus open-loop cases, we assume the values of L and C employed previously: $L = 0.01\ \text{cm H}_2\text{O s}^2\ \text{L}^{-1}$ and $C = 0.1\ \text{L cm H}_2\text{O}^{-1}$. To ensure that the condition described by Equation (4.29) is met in both open-loop and closed-loop conditions, we set $R = 1\ \text{cm H}_2\text{O s L}^{-1}$. Since the "tails" of the impulse responses will be dominated by the contribution with the longer time constant, we will compare only the values of τ_1 for open-loop versus closed-loop conditions. Applying Equation (4.34a), we find that in the open-loop situation, τ_1 is approximately 0.09 s, while in the closed-loop condition, it is approximately 0.04 s. This comparison is shown in Figure

4.4d. Therefore, as the previous cases considered, closing the loop here also increases the speed of response of the system.

4.3.2 Step Responses

To determine the response of our lung mechanics model to a unit step change in P_{ao}, we could apply the same approach that was employed for calculating the step response of the first-order model. However, for illustrative purposes, we will proceed along a somewhat different path by making use of the results that were derived for the impulse response of the second-order model. The basic principle employed here is the equivalence between multiplication in the Laplace domain and convolution in the time domain (Section 2.7). Thus, the step response, represented in the Laplace domain as

$$P_A(s) = \frac{1}{LCs^2 + RCs + \lambda} \frac{1}{s} \tag{4.35}$$

can be evaluated in the time domain from

$$g_2(t) = \int_0^t h_2(\sigma)u(t - \sigma)\, d\sigma \tag{4.36}$$

where

$$\begin{aligned} u(t) &= 1, \qquad t > 0 \\ &= 0, \qquad t \leq 0 \end{aligned} \tag{4.37}$$

and $h(t)$ represents the impulse response of the model. Inserting Equation (4.37) into Equation (4.36), the step response can be evaluated as follows:

$$g_2(t) = \int_0^t h(\sigma)\, d\sigma \tag{4.38}$$

The expression shown in Equation (4.38) implies that the step response can be evaluated by integrating the impulse response with respect to time.

4.3.2.1. Undamped Behavior. Integrating Equation (4.17) with respect to time, we obtain:

$$g_2(t) = -\frac{1}{\lambda} \cos\left(\sqrt{\frac{\lambda}{LC}}\, t\right) + A \tag{4.39a}$$

where A is an arbitrary constant. Imposing the initial condition $P_A(0) = 0$ on Equation (4.39a), we obtain the step response for undamped conditions:

$$g_2(t) = \frac{1}{\lambda}\left[1 - \cos\left(\sqrt{\frac{\lambda}{LC}}\, t\right)\right] \tag{4.39b}$$

As in the case for the impulse response, the step input elicits a sustained oscillation when there is no resistance in the system. Closing the loop increases the frequency of the oscillation but decreases its amplitude. These responses are shown in Figure 4.5a.

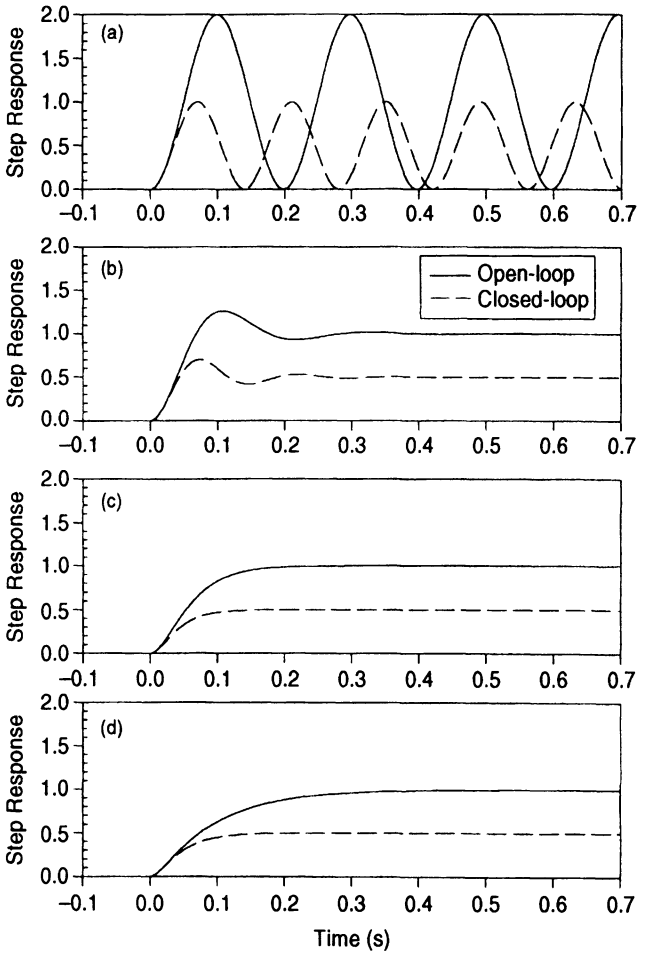

Figure 4.5 Responses of the second-order lung mechanics model to a unit step under open-loop (solid lines) and closed-loop (dashed lines) modes: (a) undamped responses; (b) underdamped responses; (c) critically damped responses; and (d) overdamped responses.

4.3.2.2. Underdamped Behavior. As in the undamped case, we obtain the step response here by convolving the impulse response described in Equation (4.23) with a unit step. This turns out to be the same as integrating the impulse response with respect to time:

$$g_2(t) = \frac{1}{LC\gamma}\int_0^t e^{-(R/2L)\sigma}\ \sin(\gamma\sigma)\, d\sigma \tag{4.40}$$

where γ is given by Equation (4.21). Performing integration by parts and imposing the initial condition that $P_A(0) = 0$, we obtain the following expression for the underdamped step response:

$$g_2(t) = \frac{1}{\lambda}\left(1 - e^{-(R/2L)t}\ \cos\gamma t - \frac{R}{2L\gamma}\ e^{-(R/2L)t}\ \sin\gamma t\right) \tag{4.41}$$

As can be seen from Figure 4.5b, the damped oscillatory characteristics of this response are the same as those of the impulse response in both open-loop and closed-loop modes.

However, in the steady state, the oscillations become fully damped out and the response settles to the constant level given by

$$g_2(t \to \infty) = \frac{1}{\lambda} \tag{4.42}$$

In Equation (4.42), note that in the open-loop case where $\lambda = 1$, the response in P_A settles down to a value of 1, i.e, the same as the unit step in P_{ao}. With the loop closed, however, where $\lambda > 1$, the steady state value of P_A is less than unity. Thus, as it was for the first-order model, the underdamped step response for the second-order model shows a *steady-state error*, ε_2, given by

$$\varepsilon_2|_{t\to\infty} = 1 - \frac{1}{\lambda} \tag{4.43}$$

4.3.2.3. Critically Damped Behavior. We obtain the critically damped response to the unit step by integrating Equation (4.27) with respect to time. After imposing the initial condition $P_A(0) = 0$, we have

$$g_2(t) = \frac{1}{LC}\left(\tau_c^2 - \tau_c(\tau_c + t)e^{-t/\tau_c}\right) \tag{4.44}$$

where τ_c is defined by Equation (4.28). The step responses for open-loop and closed-loop conditions are displayed in Figure 4.5c. As in the case for the corresponding impulse responses, closing the loop leads to a smaller τ_c and thus faster speed of response. In the steady state, as $t \to \infty$, Equation (4.44) becomes

$$g_2(t \to \infty) = \frac{\tau_c^2}{LC} = \frac{1}{\lambda} \tag{4.45}$$

where the second part of the above equation is derived by using Equation (4.28) to substitute for τ_c. Thus, the steady-state response to a unit step and the corresponding steady-state error in the critically damped mode are the same as those in the underdamped mode.

4.3.2.4. Overdamped Behavior. For the overdamped response to the unit step, we integrate Equation (4.27) with respect to time and impose the initial condition $P_A(0) = 0$ to obtain

$$g_2(t) = \frac{1}{\mu RC}\left[\tau_1(1 - e^{-t/\tau_1}) - \tau_2(1 - e^{-t/\tau_2})\right] \tag{4.46}$$

As in the critically damped case, introducing negative feedback increases the speed of response. In the steady state, as $t \to \infty$, we obtain the following result:

$$g_2(t \to \infty) = \frac{\tau_1 - \tau_2}{\mu RC} \tag{4.47a}$$

By substituting for τ_1 and τ_2 in Equation (4.47a) and employing the definition of μ given in Equation (4.31), it can be shown that this equation reduces to

$$g_2(t \to \infty) = \frac{1}{\lambda} \tag{4.47b}$$

Closing the loop gives rise to a steady-state error of the same magnitude as in the previous step responses. Open- and closed-loop overdamped responses to the unit step are compared in Figure 4.5d.

4.4 DESCRIPTORS OF IMPULSE AND STEP RESPONSES

4.4.1 Generalized Second-Order Dynamics

The impulse and step responses of both first-order and second-order lung mechanics models have demonstrated that when proportional feedback is introduced, alveolar pressure changes resulting from perturbations in P_{ao} (the input) are attenuated. The resulting fluctuations in P_A also respond more quickly to changes in P_{ao} under closed-loop conditions.

In the various impulse and step responses derived for the lung mechanics model in Section 4.3, it should be pointed out that although the model contained three physiological parameters (L, C, and R), these parameters always appeared in combination with one another, e.g., LC and RC. Indeed, the transfer function $P_A(s)/P_{ao}(s)$ contains only two free parameters for a given value of k, the feedback gain; thus, more than one combination of R, C, and L may produce the same dynamics. In this section, we will present the system equations for a generalized second-order model that is characterized by the same dynamics as the lung mechanics model. In the generalized model, the second-order dynamics are governed by two independent parameters. A third parameter, the steady-state input–output gain, G_{SS}, is also introduced. In the particular example of the lung mechanics model, G_{SS} turned out to be unity. In addition, we generalize the input and output to be $x(t)$ and $y(t)$. Then, denoting the Laplace transforms of $x(t)$ and $y(t)$ by $X(s)$ and $Y(s)$, respectively, we can convert Equation (4.5a) to

$$\frac{Y(s)}{X(s) - kY(s)} = \frac{G_{SS}}{LCs^2 + RCs + 1} \tag{4.48}$$

We can generalize Equation (4.48) further by introducing two new parameters to substitute for the three redundant parameters, R, L, and C. It will soon become obvious that these two new parameters provide a highly intuitive description of the dynamic properties of the model. We begin by considering the undamped open-loop system ($k = 0$). As we had shown earlier, the responses to unit impulse or step took the form of a sustained oscillation. In fact, the angular frequency of the oscillation represents the highest frequency at which the system will "resonate." This frequency is commonly referred to as the *natural frequency*, ω_n. From Equation (4.17), we find that ω_n is defined by

$$\omega_n = \frac{1}{\sqrt{LC}} \tag{4.49}$$

The second new parameter that we will introduce is ζ, defined as

$$\zeta = \frac{R}{2}\sqrt{\frac{C}{L}} \tag{4.50}$$

Substituting Equations (4.49) and (4.50) into Equation (4.48) and rearranging terms, it can be easily shown that the overall transfer function for the model now becomes

$$\frac{Y(s)}{X(s)} = \frac{G_{SS}\omega_n^2}{s^2 + 2\zeta\omega_n s + (1 + kG_{SS})\omega_n^2} \tag{4.51}$$

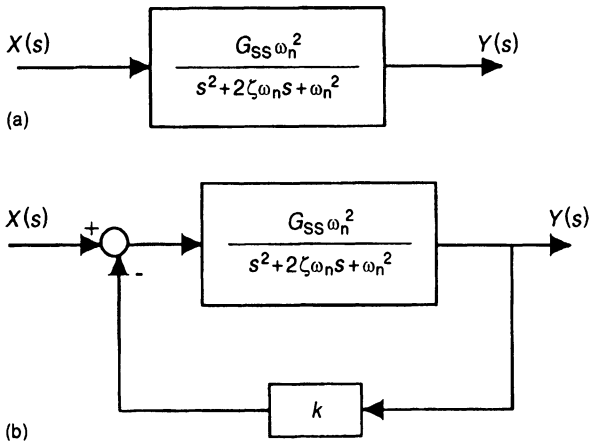

Figure 4.6 (a) Generalized second-order open loop model. (b) Generalized second-order closed-loop model.

The open-loop and closed-loop versions of this generalized system are depicted schematically in Figures 4.6a and 4.6b, respectively.

Whether the resulting impulse or step responses are undamped, underdamped, critically damped or overdamped depends on the roots of the denominator in Equation (4.51). It can be seen that this, in turn, depends on the value of the parameter, ζ. Note that when $\zeta = 0$, the impulse or step response will be a sustained oscillation. In the open-loop case, when $0 < \zeta < 1$, the impulse and step responses will show damped oscillatory behavior. However, when $\zeta \geq 1$, these responses will assume an exponential form. It is clear that ζ represents the amount of "damping" inherent in the system and, for this reason, it is commonly referred to as the *damping factor* or *damping ratio*.

4.4.1.1. Undamped Dynamics. In the case when $\zeta = 0$, Equation (4.51) becomes

$$\frac{Y(s)}{X(s)} = \frac{G_{SS}\omega_n^2}{s^2 + (1 + kG_{SS})\omega_n^2} \tag{4.52}$$

The inverse Laplace transform of Equation (4.52) yields an oscillatory solution for the impulse response, $h_2(t)$:

$$h_2(t) = \frac{G_{SS}\omega_n}{\sqrt{1 + kG_{SS}}} \sin\left(\sqrt{1 + kG_{SS}}\omega_n t\right) \tag{4.53}$$

The step response, $g_2(t)$, which is also oscillatory, is obtained by integrating $h_2(t)$ with respect to time:

$$g_2(t) = \frac{G_{SS}}{1 + kG_{SS}} \left(1 - \cos\left(\sqrt{1 + kG_{SS}}\omega_n t\right)\right) \tag{4.54}$$

Note from Equation (4.54) that the step response oscillates around the constant level $G_{SS}/(1 + kG_{SS})$.

4.4.1.2. Underdamped Dynamics. In the underdamped mode, when $\zeta^2 < 1 + kG_{SS}$, the denominator in Equation (4.51) can be rearranged so that the following form is obtained:

$$\frac{Y(s)}{X(s)} = \frac{G_{SS}\omega_n^2}{(s + \zeta\omega_n)^2 + \omega_n^2(1 + kG_{SS} - \zeta^2)} \tag{4.55}$$

The impulse response corresponding to Equation (4.55) is

$$h_2(t) = \frac{G_{SS}\omega_n}{\sqrt{1 + kG_{SS} - \zeta^2}} e^{-\omega_n \zeta t} \sin\left(\omega_n \sqrt{1 + kG_{SS} - \zeta^2}\, t\right) \tag{4.56}$$

while the step response is

$$g_2(t) = \frac{G_{SS}}{1 + kG_{SS}} \left(1 - \frac{e^{-\zeta\omega_n t}}{\sqrt{1 + kG_{SS} - \zeta^2}} \sin\left(\omega_n \sqrt{1 + kG_{SS} - \zeta^2}\, t + \theta\right)\right) \tag{4.57}$$

where

$$\theta = \tan^{-1}\left(\sqrt{\frac{1 + kG_{SS} - \zeta^2}{\zeta}}\right)$$

4.4.1.3. Critically Damped Dynamics. The roots of the denominator become real and equal when $\zeta^2 = 1 + kG_{SS}$. At this point, all oscillatory dynamics disappear and the system becomes "critically damped." Equation (4.51) becomes

$$\frac{Y(s)}{X(s)} = \frac{G_{SS}\omega_n^2}{(s + \zeta\omega_n)^2} \tag{4.58}$$

The impulse response that corresponds to Equation (4.58) is

$$h_2(t) = G_{SS}\omega_n^2 t e^{-\omega_n t} \tag{4.59}$$

while the step response is

$$\begin{aligned} g_2(t) &= \frac{G_{SS}}{\zeta}\left[\frac{1}{\zeta} - \left(\frac{1}{\zeta} + \omega_n t\right)e^{-\zeta\omega_n t}\right] \\ &= \frac{G_{SS}}{\sqrt{1 + kG_{SS}}}\left[\frac{1}{\sqrt{1 + kG_{SS}}} - \left(\frac{1}{\sqrt{1 + kG_{SS}}} + \omega_n t\right)e^{-\zeta\omega_n t}\right] \end{aligned} \tag{4.60}$$

4.4.1.4. Overdamped Dynamics. When ζ^2 exceeds $1 + kG_{SS}$, the roots of the denominator of Equation (4.51) become real and different, so that the corresponding impulse and step responses now become

$$h_2(t) = \frac{G_{SS}\omega_n}{2\sqrt{\zeta^2 - 1 - kG_{SS}}}\left(e^{-\omega_n(\zeta - \sqrt{\zeta^2 - 1 - kG_{SS}})t} + e^{-\omega_n(\zeta + \sqrt{\zeta^2 - 1 - kG_{SS}})t}\right) \tag{4.61}$$

$$g_2(t) = \frac{G_{SS}}{2\sqrt{\zeta^2 - 1 - kG_{SS}}}\left(\frac{1 - e^{-\omega_n(\zeta - \sqrt{\zeta^2 - 1 - kG_{SS}})t}}{\zeta - \sqrt{\zeta^2 - 1 - kG_{SS}}} + \frac{1 - e^{-\omega_n(\zeta + \sqrt{\zeta^2 - 1 - kG_{SS}})t}}{\zeta + \sqrt{\zeta^2 - 1 - kG_{SS}}}\right) \tag{4.62}$$

4.4.1.5. Steady-State Error. In the underdamped, critically damped and overdamped modes of the generalized second-order system, the step response attains the same steady-state value. In Equations (4.57) and (4.60), we can deduce this final value easily by letting t tend to

infinity. The same can be done for the overdamped mode in Equation (4.62), except that a little algebra will be needed to obtain the following expression for the steady-state response:

$$g_2(t \to \infty) = \frac{G_{SS}}{1 + kG_{SS}} \tag{4.63}$$

The steady-state error is deduced by subtracting the steady-state response from the input value, which is unity since the unit step was employed. Under open-loop circumstances ($k = 0$), the steady-state error would be

$$\varepsilon_2|_{\text{open-loop}} = 1 - G_{SS} \tag{4.64}$$

Note that, in the special case when $G_{SS} = 1$, as in the example considered in Section 4.3.2, the open-loop steady-state error is zero. However, when G_{SS} assumes other values, the open-loop steady-state error can be quite large. In the closed-loop case, the steady state error is given by

$$\varepsilon_2|_{\text{closed-loop}} = 1 - \frac{G_{SS}}{1 + kG_{SS}} \tag{4.65}$$

In the special case where $G_{SS} = 1$, the steady-state error becomes $k/(1 + k)$, as was previously shown in the example in Section 4.3.2.

4.4.2 Transient Response Descriptors

The first-order and second-order impulse and step responses we have discussed constitute the simplest approximations to the corresponding time-domain dynamics of real physiological systems. To characterize more realistic impulse and step responses, one could in principle extend the modeling analysis to higher-order models. But as this process continues, the mathematics rapidly become less and less tractable. Furthermore, the number of parameters needed to describe these responses will also increase. In some situations, it may be necessary to compare the dynamic behavior of one system with that of another. Alternatively, one may need to compare the dynamic characteristics of the same system under different conditions. In order to do this, it is possible to first estimate the impulse and/or step responses, and then extract certain descriptors from these responses empirically. Subsequently, standard statistical analyses, such as the Student t-test, can be employed to determine whether the two sets of dynamic responses are significantly different from one another. The descriptors discussed below are among the most commonly used in systems analysis.

4.4.2.1. Impulse Response Descriptors. These descriptive features of the impulse response are illustrated in Figure 4.7a. The most direct feature is the *peak amplitude*, which simply measures the maximum (or minimum, if the response is predominantly negative) value of the impulse response. Thus,

$$\text{Peak Amplitude} = \max[h(t)] \quad \text{or} \quad |\min[h(t)]| \tag{4.66}$$

The *area* under the impulse response function represents the integral of $h(t)$ over time, which in turn yields the *steady-state gain*, G_{SS}, of the system:

$$G_{SS} = \int_{-\infty}^{\infty} h(t)\, dt \tag{4.67}$$

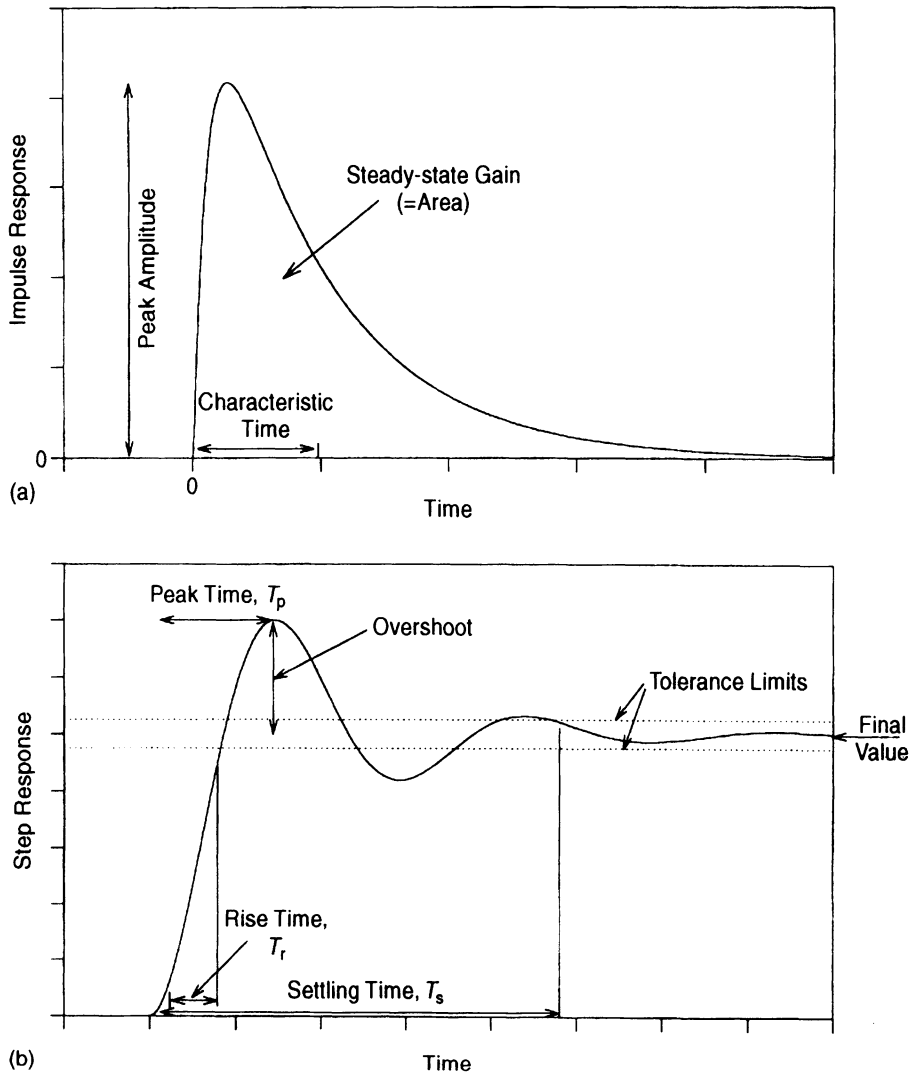

Figure 4.7 Descriptors of (a) the impulse response and (b) the step response.

Finally, the *characteristic time*, T_c, provides a measure of the approximate latency following which the bulk of the impulse response occurs. Alternatively, T_c may also be thought of in the following way. If the impulse response function is represented as a two-dimensional mass, then T_c will be the location (on the time axis) at which the center of mass acts:

$$T_c = \frac{\int_{-\infty}^{\infty} t\,|h(t)|\,dt}{\int_{-\infty}^{\infty} |h(t)|\,dt} \tag{4.68}$$

4.4.2.2. Step Response Descriptors. The most commonly used descriptors of the step response are shown in Figure 4.7b. As mentioned previously, the *final value* of the response is the steady-state level achieved by the system in question. If the input is a *unit step*, this final value will yield the steady-state gain, G_{SS}. If the peak value of the step response is larger than

the final value, the *overshoot* will be the difference between this peak value and the final value. Frequently, this overshoot is expressed in percentage terms:

$$\text{Percent Overshoot} = \frac{\text{Peak Response} - \text{Final Value}}{\text{Final Value}} \times 100\% \tag{4.69}$$

The time taken for the step response to achieve its peak value is known as the *peak time*, or T_p as illustrated in Figure 4.7b. Aside from peak time, there are two other measures of speed of response. One is the *rise time*, T_r, defined as

$$T_r = t_{90\%} - t_{10\%} \tag{4.70}$$

where $t_{90\%}$ = time at which response first achieves 90% of its final value, $t_{10\%}$ = time at which response first achieves 10% of its final value.

The other measure of speed of response is the settling time, T_s, defined as the time taken for the step response to settle within $\pm\delta\%$ of the final value. The upper and lower levels of this band of values, i.e. $100 + \delta\%$ and $100 - \delta\%$ of the final value, define the tolerance limits within which the step response will remain at all times greater than T_s. The values of δ generally employed range from 1% to 5%.

4.5 OPEN-LOOP VERSUS CLOSED-LOOP DYNAMICS: OTHER CONSIDERATIONS

4.5.1 Reduction of the Effects of External Disturbances

In our previous discussions of the first-order and second-order models of lung mechanics, we showed that one clear consequence of introducing negative feedback into the control scheme is *an increase in speed of system response.* A second major effect of closing the loop is the reduction in overall system gain. For both first-order and second-order models, closing the loop led to a significant reduction of the final values in the unit step responses (see Figures 4.3b and 4.5). This result is consistent with the conclusion that we arrived at in Section 3.2, although those considerations were based entirely on steady-state conditions. As we had pointed out in that section, what is most advantageous about this reduction in overall system gain is the enhanced ability of the closed-loop system to attenuate the impact of external disturbances. To emphasize the importance of this point, we will consider a simple example here.

Figures 4.8a and 4.8b illustrate the open-loop and closed-loop versions of a generalized linear control system. $D(s)$ represents the Laplace transform of an external disturbance that contributes "noise" directly and additively to the output. Thus, in the open-loop case,

$$Y(s) = G(s)X(s) + D(s) \tag{4.71}$$

which clearly shows that 100% of the external disturbance is reflected in the output. However, in the closed-loop case, we have

$$Y(s) = G(s)[X(s) - H(s)Y(s)] + D(s) \tag{4.72a}$$

which, upon rearranging terms, becomes:

$$Y(s) = \frac{G(s)}{1 + G(s)H(s)} X(s) + \frac{1}{1 + G(s)H(s)} D(s) \tag{4.72b}$$

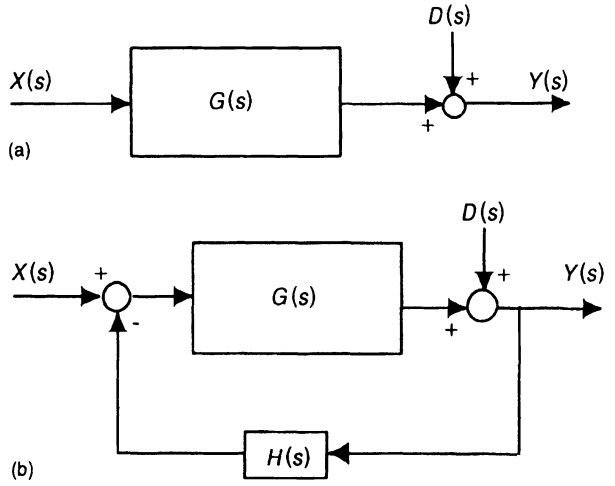

Figure 4.8 (a) Generalized linear open-loop system. (b) Generalized linear closed-loop system.

Since we have explicitly incorporated negative feedback into the equations, the common denominator in Equation (4.72b) satisfies the following condition:

$$|1 + G(s)H(s)| > 1 \tag{4.73}$$

As such, the effect of $D(s)$ on $Y(s)$ will be attenuated and can be further attenuated as we increase the magnitude of the product $G(s)H(s)$, which is the *loop gain* (*LG*) of the closed-loop system.

4.5.2 Reduction of the Effects of Parameter Variations

There are situations, particularly when dealing with the artificial control of some physiological variable, where there may be a need to decide upon a range of the input $x(t)$ signal in order to closely regulate variations in the output $y(t)$. This can only be done if we have a very good idea of the characteristics of the feedforward subsystem $G(s)$. However, this may not always be possible, as we may have erroneous estimates of $G(s)$ or $G(s)$ may actually be time-varying. These variations in the system parameters will have an impact on the controlled output.

First, consider the open-loop case. Assume that there is a small change in the transfer characteristics of $G(s)$, which we will denote by $\Delta G(s)$. Then, the effect on the output will be

$$Y(s) + \Delta Y(s) = [G(s) + \Delta G(s)]X(s) + D(s) \tag{4.74}$$

Eliminating the equivalent expression for $Y(s)$, we can derive the following:

$$\Delta Y(s) = \Delta G(s)X(s) \tag{4.75}$$

The above result shows that the variation in $G(s)$ is directly reflected in the output. Now, consider the corresponding result as we apply the same type of analysis to the closed-loop system:

$$Y(s) + \Delta Y(s) = D(s) + [G(s) + \Delta G(s)]\{X(s) - H(s)[Y(s) + \Delta Y(s)]\} \tag{4.76}$$

Again, we expand Equation (4.76) and eliminate $Y(s)$ from both sides of the equation. We also eliminate the term containing the product of differences $\Delta G(s)$ and $\Delta Y(s)$, since we have assumed these differences to be small. These steps lead to the following result:

$$\Delta Y(s) = \frac{\Delta G(s)}{[1 + G(s)H(s)]^2} X(s) \tag{4.77}$$

Thus, in the closed-loop case, the effect of $\Delta G(s)$ is reduced by a factor of $[1 + G(s)H(s)]^2$.

4.5.3 Integral Control

In spite of the many advantages of employing proportional feedback control, one problem that can be highly aggravating in some applications is the existence of the steady-state error. We will demonstrate in this section that the steady-state error can be eliminated completely by employing integral control. To understand how this can be achieved, consider the proportional control and integral control systems shown in Figures 4.9a and 4.9b, respectively.

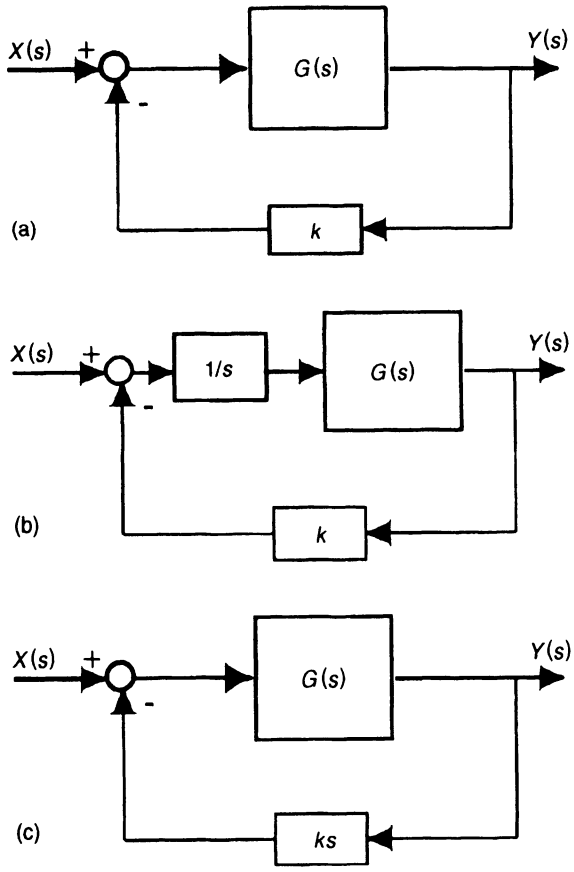

Figure 4.9 Different closed-loop control schemes: (a) proportional feedback control; (b) integral control; (c) derivative feedback control.

First consider the proportional control system shown. This represents a generalization of the particular first-order and second-order models discussed in Sections 4.2 and 4.3. The Laplace transform of the difference (error) between the input and output is given by

$$E(s) = X(s) - Y(s) = \left(1 - \frac{G(s)}{1 + kG(s)}\right) X(s) \tag{4.78}$$

The steady-state error, $e(t \to \infty)$, can be deduced from the above equation by using the unit step input (i.e., setting $X(s) = 1/s$) and evaluating the result via the Final Value Theorem for Laplace transforms:

$$e(t \to \infty) = \lim_{s \to 0} sE(s) \tag{4.79}$$

Applying Equation (4.79) to Equation (4.78), we obtain

$$e(t \to \infty) = \frac{1 + (k - 1)G_{SS}}{1 + kG_{SS}} \tag{4.80}$$

where G_{SS} here represents the steady-state value of $G(s)$. Note that we can minimize the steady-state error by setting k equal to unity, in which case:

$$e(t \to \infty)_{\min} = \frac{1}{1 + G_{SS}} \tag{4.81}$$

Now consider the case for integral control, in which the error signal is integrated prior to being used to drive the actuator (plant) portion of the closed-loop system. In this case, the Laplace transform of the difference between input and output is

$$E(s) = X(s) - Y(s) = \left(1 - \frac{G(s)}{s + kG(s)}\right) X(s) \tag{4.82}$$

Using Equation (4.79), and assuming the input to be a unit step ($X(s) = 1/s$), we obtain

$$e(t \to \infty) = \frac{(k - 1)G_{SS}}{kG_{SS}} \tag{4.83}$$

In this case, we can eliminate the steady-state error completely by setting k to unity. However, this advantage of not having a steady-state error is derived at the expense of speed of system response.

For a more intuitive explanation of why there is always a steady-state error in proportional feedback control but not in integral control, consider both cases when $k = 1$. In proportional control, if the steady-state error ($e(t \to \infty) = x(t \to \infty) - y(t \to \infty)$) is zero, this would also make the error signal that drives the actuator/plant zero, which in turn implies that the steady-state output $y(t \to \infty)$ would become zero. This result would be incompatible with the prior assertion that $e(t \to \infty)$ is zero, since $x(t \to \infty)$ equals unity. Thus, for the proportional feedback system, *a steady-state error must exist* in order for the system to produce a nonzero output. Now consider the integral control scheme. Assume that, before time zero, both input and output are zero. When the unit step takes effect at the input, $y(t)$ will initially remain at zero and consequently, there will be a large error signal that feeds into the integrator. However, with time, as $y(t)$ increases toward its final value, this error signal will diminish. On the other hand, the output of the integrator will remain high since it represents the accumulation of all previous values of the error signal. Finally, when $y(t \to \infty)$ attains the same value as $x(t \to \infty)$, the steady-state error will become zero, and the

integrator output, which drives the actuator/plant, will cease increasing but remain at its final positive value so that $y(t \to \infty)$ will be unchanged (and equal to $x(t \to \infty)$).

4.5.4 Derivative Feedback

Instead of feeding back a signal directly proportional to the system output, how would closed-loop dynamics be different if the feedback signal were proportional to the *time-derivative* of the output? Consider the control scheme illustrated in Figure 4.9c and, for the sake of simplicity, let us assume in this example that

$$G(s) = \frac{1}{\tau s + 1} \tag{4.84}$$

Then,

$$\frac{Y(s)}{X(s) - ksY(s)} = \frac{1}{\tau s + 1} \tag{4.85}$$

From Equation (4.85), we derive the following expression for the overall system transfer function:

$$\frac{Y(s)}{X(s)} = \frac{1}{\tau' s + 1} \tag{4.86}$$

where

$$\tau' = \tau + k \tag{4.87}$$

The unit step response corresponding to Equations (4.86) and (4.87) is

$$g_1(t) = 1 - e^{-(t/\tau + k)} \tag{4.88}$$

It is clear from this result that derivative feedback increases the effective time constant and therefore produces a more sluggish response. In other words, derivative feedback increases system damping.

To determine how derivative feedback affects steady-state error, we derive from Equation (4.86) the following expression:

$$E(s) = X(s) - Y(s) = \left(1 - \frac{1}{\tau' s + 1}\right) X(s) \tag{4.89}$$

Then, using Equation (4.79), the steady-state error is found to be

$$e(t \to \infty) = \lim_{s \to 0} \left[s \left(1 - \frac{1}{\tau' s + 1}\right) \frac{1}{s} \right] = 0 \tag{4.90}$$

Thus, derivative feedback of the kind shown in Figure 4.9c leads to the elimination of the steady-state error.

There is a popular variant of this type of control known as "velocity feedback," in which the feedback signal consists of the sum of a term proportional to the output and a term proportional to the derivative of the output. In this case, there will in general be a steady-state error. However, the steady-state error can be attenuated by increasing the gain of the forward block, G_{SS}. In the limit, when $G_{SS} \to \infty$, the steady-state error will become zero.

4.6 TRANSIENT RESPONSE ANALYSIS USING MATLAB

If the form of the transfer function of a given model is known, the response of the system to standard inputs, such as the unit impulse or unit step, as well as any arbitrary input waveform, can be deduced easily in MATLAB. The following MATLAB command lines (also found in the script file `tra_llm.m`) demonstrate how transient response analysis can be applied to the linearized lung mechanics model that we have been discussing.

Assuming that the parameter values of L, R, C, and k in Equation (4.5b) have been preassigned, we begin by setting up the transfer function, `Hs`, of the model:

```
>> num = [1]
>> den = [L*C R*C 1 + k];
>> Hs = tf(num,den;
>> t=[0:0.005:0.8];
```

The first two lines assign values to the various terms in the numerator (`num`) and denominator (`den`) of `Hs`. In the case of the denominator, these values are assigned in the order of descending powers of s. The fourth line simply generates a time vector covering the duration of the response that we will examine.

The impulse response is computed and plotted using the following command lines:

```
>> x = impulse (Hs, t);
>> plot(t,x)
```

The command lines that follow produce a plot of the unit step response:

```
>> y = step (Hs, t);
>> plot(t,y)
```

Finally, the response of this system to an input, u, of arbitrary time-course can be computed using the `lsim` function:

```
>> [u, t] = gensig('square',0.5,5,0.005);
>> y = lsim (Hs, u, t);
>> plot(t,y)
```

In this example, the "arbitrary input" is a square wave of period 0.5 s, lasting up to time $t = 5$ s (in time steps of 0.005 s), generated with the function "`gensig`."

4.7 SIMULINK APPLICATION: DYNAMICS OF NEUROMUSCULAR REFLEX MOTION

Up to this point, we have limited our analyses to simple models with only first-order or second-order dynamics. This was done intentionally to demonstrate the methodology

employed in classical time-domain analysis without letting the mathematical details become too intractable and distracting. To extend this kind of analysis to more complex (and more realistic) physiological models, it becomes progressively more convenient to employ the methods of computer simulation. In this section, we will demonstrate an example of time-domain analysis using SIMULINK.

4.7.1 A Model of Neuromuscular Reflex Motion

Examination of the dynamics of neuromuscular reflex motion can yield valuable insight into the status of patients who have neurological disorders. The model that we will consider assumes the following test. The patient is seated comfortably and his shoulder and elbow are held by adjustable supports so that the upper arm remains in a fixed horizontal position throughout the test. The subject's forearm is allowed to move only in the vertical plane. At the start of the experiment, he is made to flex his arm by pulling on a cord that has been attached to a cuff on his wrist. The cord runs around a pulley system and supports a sizeable weight. The initial angle between the forearm and upper arm is 135°. The subject is not given any specific instructions about maintaining this angle, except to relax his arm as much as possible while supporting the weight. Then, at time $t = 0$, an electromagnetic catch is switched off so that an additional weight is abruptly added to the original load. Changes in angular motion, $\theta(t)$, of the forearm about the elbow are recorded during and after the quick release of the weight. The mathematical model used to interpret the results of this test is based on the work of Soechting et al. (1971).

4.7.1.1. Limb Dynamics. Figure 4.10a shows a schematic diagram of the forearm, with the black filled circle representing the elbow joint. M_x represents the change in external moment acting on the limb about the elbow joint; in this experiment, M_x would be a step. M represents the net muscular torque exerted in response to the external disturbance. Neglecting the weight of the forearm itself, application of Newton's Second Law yields the following equation of motion:

$$M_x(t) - M(t) = J\ddot{\theta} \tag{4.91}$$

where J is the moment of inertia of the forearm about the elbow joint.

4.7.1.2. Muscle Model. Although this reflex involves both the biceps and triceps muscles, we will assume for simplicity that the net muscular torque in response to M_x is generated by a single equivalent muscle model, illustrated in Figure 4.10b. Note that in this mechanical analog, M is treated as if it were a "force," although it is actually a torque. Accordingly, the "displacements" that result are in fact angular changes, θ and θ_1. As such, the muscle stiffness parameter, k, and the viscous damping parameter, B, have units consistent with this representation. The equations of motion for the muscle model are:

$$M(t) = k(\theta - \theta_1) \tag{4.92}$$

and

$$M(t) = M_0(t) + B\dot{\theta}_1 \tag{4.93}$$

where $M_0(t)$ is the torque exerted by the muscle under isometric conditions. $M_0(t)$ is represented as a function of time, since it is dependent on the pattern of firing of the alpha motorneurons.

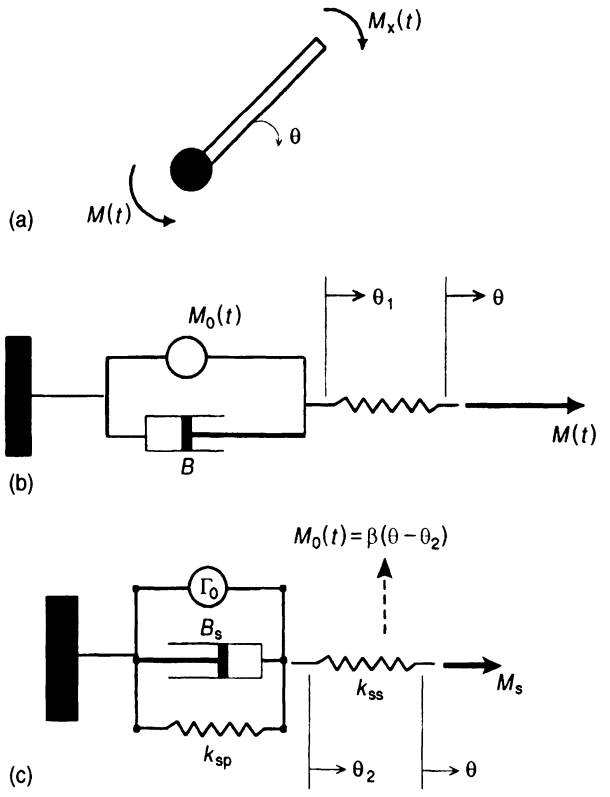

Figure 4.10 Components of the neuromuscular reflex model: (a) limb dynamics; (b) muscle model; (c) muscle spindle model.

4.7.1.3. Plant Equations. By combining Equations (4.91) through (4.93), we obtain an equation of motion that characterizes the dynamics of the plant, i.e., describing how θ would change due to the torque exerted by the external disturbance M_x and the resulting muscular response:

$$\frac{BJ}{k}\dddot{\theta} + J\ddot{\theta} + B\dot{\theta} = M_x(t) - M_0(t) \tag{4.94}$$

4.7.1.4. Muscle Spindle Model. This model describes the dynamics by which changes in θ are transduced at the level of the muscle spindles into afferent neural signals. The latter travel to the spinal cord, which sends out efferent signals to the contractile machinery of the muscle to generate $M_0(t)$. We assume that the neural output of the spindle is proportional to the amount by which its nuclear bag region is stretched, so that ultimately

$$M_0(t) = \beta(\theta - \theta_2) \tag{4.95}$$

Figure 4.10c shows the mechanical analog of the muscle spindle model. k_{sp} and B_s are parameters that represent the elastic stiffness and viscous damping properties, respectively, of the pole region of the spindle, while k_{ss} represents the elastic stiffness of the nuclear bag region. Γ_0 represents the contractile part of the pole region, which allows the operating length of the spindle to be reset at different levels, using the gamma motorneuronal pathways. We

will assume Γ_0 to be constant at the equilibrium length of the spindle, so that this parameter does not play a role in the dynamics of changes about this equilibrium length. With this consideration in mind, the dynamics of the muscle spindle model may be characterized by the following equations:

$$M_s = K_{ss}(\theta - \theta_2) \tag{4.96}$$

and

$$M_s = B_s\dot{\theta}_2 + k_{sp}\theta_2 \tag{4.97}$$

Another important factor that must be taken into account is the fact that, although θ is sensed virtually instantaneously by the spindle organs, there is a finite delay before this feedback information is finally converted into corrective action at the level of the muscle. This total delay, T_d, includes all lags involved in neural transmission along the afferent and efferent pathways as well as the delay taken for muscle potentials to be converted into muscular force. Eliminating the intermediate variables, M_s and θ_2, from Equations (4.95) through (4.97), we obtain the following equation for the feedback portion of the stretch reflex model:

$$M_0 + \frac{M_0}{\tau} = \beta\left(\dot{\theta}(t - T_d) + \frac{\theta(t - T_d)}{\eta\tau}\right) \tag{4.98}$$

where

$$\tau = \frac{B_s}{k_{ss} + k_{sp}} \tag{4.99}$$

and

$$\eta = \frac{k_{ss} + k_{sp}}{k_{sp}} \tag{4.100}$$

4.7.1.5. Block Diagram of Neuromuscular Reflex Model. Taking the Laplace transforms of Equations (4.94) and (4.98), we obtain the following equations that are represented schematically by the block diagram shown in Figure 4.11:

$$\theta(s) = \frac{M_x(s) - M_0(s)}{s\left(\frac{BJ}{k}s^2 + Js + B\right)} \tag{4.101}$$

and

$$M_0(s) = \beta\frac{\tau s + 1/\eta}{\tau s + 1}\, e^{-sT_d}\theta(s) \tag{4.102}$$

4.7.2 SIMULINK Implementation

The SIMULINK implementation of the neuromuscular reflex model is depicted in Figure 4.12. This program has been saved as the file "`nmreflex.mdl`." Note that the model parameters appear in the program as variables and not as fixed constants. This gives us the flexibility of changing the parameter values by entering them in the MATLAB command window or running a MATLAB m-file immediately prior to running the SIMULINK program. In this case, we have chosen the latter path and created an m-file called

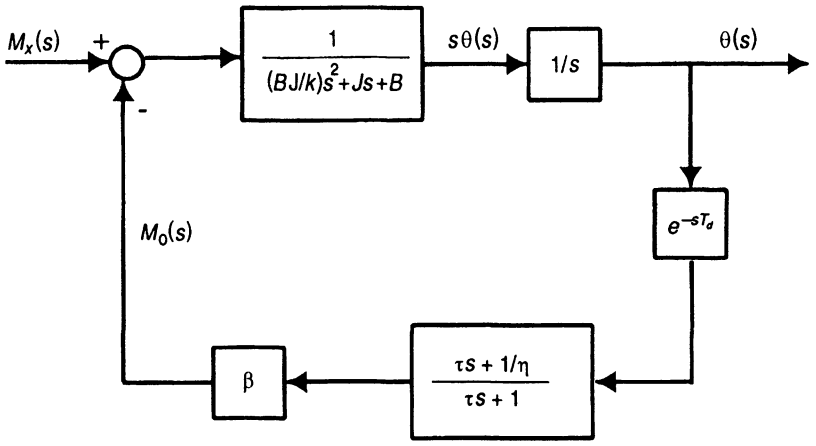

Figure 4.11 Block diagram of neuromuscular reflex model.

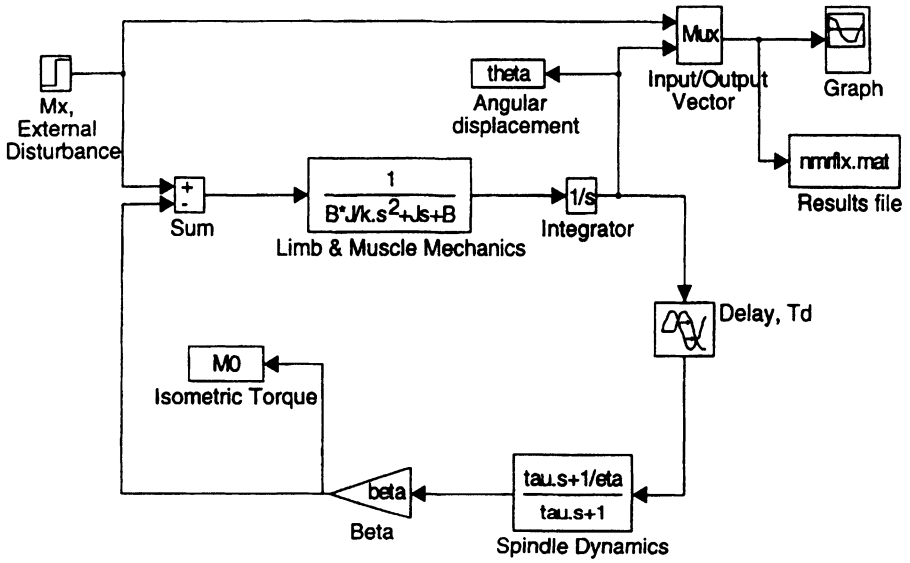

Figure 4.12 SIMULINK implementation of neuromuscular reflex model.

"`nmr_var.m`" that specifies the parameter values. The nominal parameter values used in the simulation are as follows: $J = 0.1\,\text{kg m}^2$, $k = 50\,\text{N m}$, $B = 2\,\text{N m s}$, $T_d = 0.02\,\text{s}$, τ ("`tau`" in Figure 4.12) = 1/300 s, η ("`eta`" in Figure 4.12) = 5, and β ("`beta`" in Figure 4.12) = 100. These values are consistent with the average physiological equivalents found in normal adult humans.

Figure 4.13 displays the results of three simulation runs with "`nmreflex.mdl`" using the nominal parameter values mentioned above. The upper panel shows the time-course of the external disturbance, M_x, which is a step increase of 5 N m in the moment applied to the forearm. The solid tracing in the lower panel represents the corresponding response in θ, the angular displacement of the forearm, when β was set equal to 100. Note that positive values of θ correspond to increases in the angle of flexion between the forearm and the upper arm. There is a slight overshoot in θ, followed by an almost undetectable oscillation before the

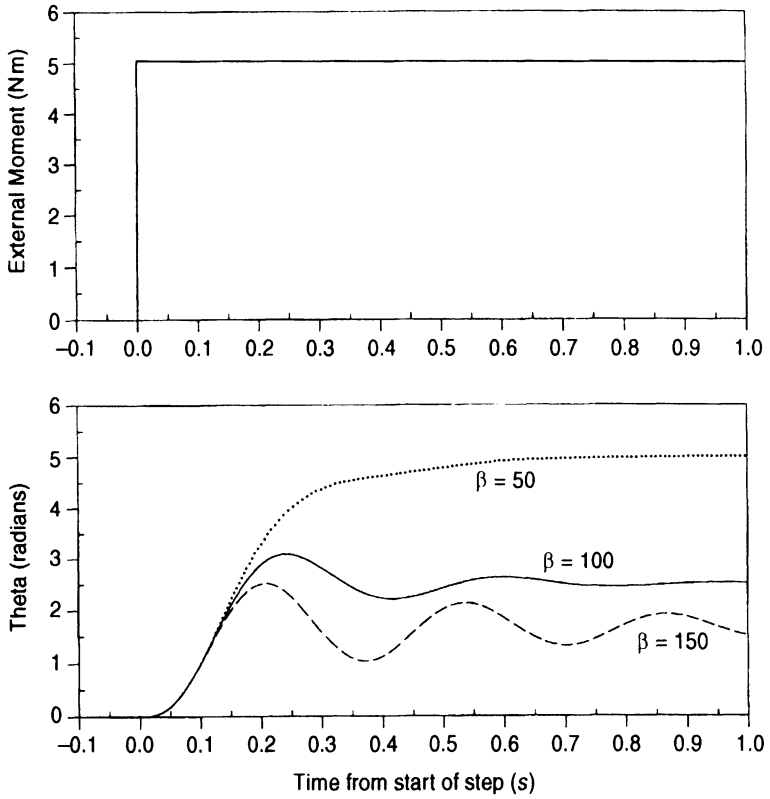

Figure 4.13 Sample results of simulations using the SIMULINK implementation of the neuromuscular reflex model.

steady-state value of approximately 0.25 radian is attained. Note that β represents the overall gain of the reflex arc. When β was increased to 150, the response was a damped oscillation, but the steady-state value achieved by θ became smaller than that obtained with the nominal value of β. In the third simulation, β was decreased to half the nominal value (i.e., 50). This produced an overdamped response and also resulted in a larger end-value for θ. These results reiterate the point that increased feedback gain leads to better attenuation of the effects of imposed disturbances—higher values of β produced smaller ending values for θ. On the other hand, the responses also become more oscillatory. This issue of instability will be discussed further in Chapter 6.

BIBLIOGRAPHY

Dorf, R.C., and R.H. Bishop. *Modern Control Systems*, 7th ed. Addison-Wesley, Reading, MA, 1995.

Dorny, C.N. *Understanding Dynamic Systems*. Prentice-Hall, Englewood Cliffs, NJ, 1993.

Jackson, A.C., and H.T. Milhorn. Digital computer simulation of respiratory mechanics. *Comput. Biomed. Res.* **6**: 27–56, 1973.

Kuo, B.C. *Automatic Control Systems*, 4th ed. Prentice-Hall, Englewood Cliffs, NJ, 1994.

Milhorn, H.T. *The Application of Control Theory to Physiological Systems*. W.B. Saunders, Philadelphia, 1966.

Milsum, J.H. *Biological Control Systems Analysis*. McGraw-Hill, New York, 1966.

Shahian, B., and M. Hassul. *Control System Design using MATLAB*. Prentice-Hall, Englewood Cliffs, NJ, 1993.

Soechting, J.F., P.A. Stewart, R.H. Hawley, P.R. Paslay, and J. Duffy. Evaluation of neuromuscular parameters describing human reflex motion. *Trans. ASME, Series G* **93**: 221–226, 1971.

Strum, R.D., and D.E. Kirk. *Contemporary Linear Systems using MATLAB*. PWS Publishing Co., Boston, MA, 1994.

PROBLEMS

P4.1. Figure P4.1 shows the block diagram of a simplified model of eye-movement control. J represents the moment of inertia of the eyeball about the axis of rotation, while B represents the viscous damping associated with the rotational movement of the eye. The target angular position of the eye, θ_{ref}, is set by the higher centers. G is a gain that converts the controlling signal into the torque exerted by the extraocular muscles. Information about the angular position of the eye, θ, is fed back to the controller with unity gain. Velocity information is also fed back with variable gain, k_v (> 0). Deduce expressions for the responses of this system to a unit step change in θ_{ref} when:

(a) there is no feedback at all;

(b) there is only position feedback ($k_v = 0$);

(c) both position and velocity feedback exist.

P4.2. Determine the response in angular displacement of the eye in Figure P4.1 if the target input θ_{ref} were to follow the trajectory of a unit ramp, i.e., $\theta_{ref} = t$ ($t > 0$). How would this ramp response be affected if the velocity feedback gain, k_v, were made negative?

P4.3. The following transfer function is one of the simplest linear approximations to the pure time delay, T:

$$H(s) = \frac{1 - \frac{Ts}{2}}{1 + \frac{Ts}{2}}$$

Determine the open-loop and closed-loop responses for the system shown in Figure P4.2 when the input is a unit step.

P4.4. Many types of physiological receptors exhibit the property of rate sensitivity. Carbon dioxide (CO_2) receptors have been found in the lungs of birds and reptiles, although it remains unclear whether such receptors are also found in human lungs. Figure P4.3 shows a highly simplified model of the way in which ventilation may be controlled by these intrapulmonary receptors following denervation of the carotid bodies. The feedforward

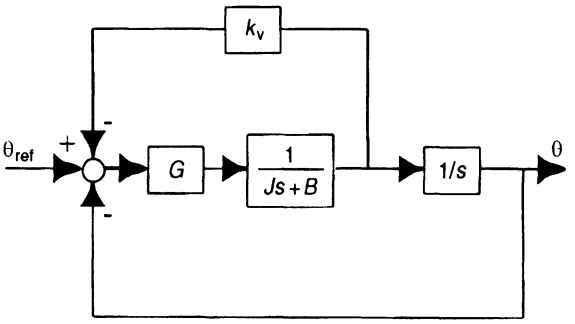

Figure P4.1 Simple model of eye-movement control.

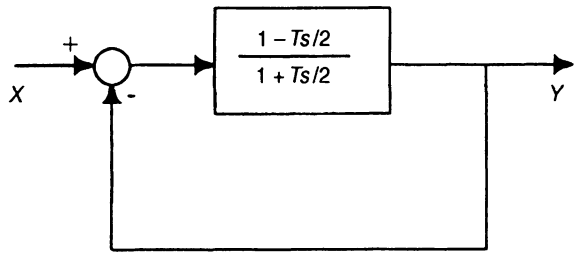

Figure P4.2 Closed-loop system containing time-delay approximation.

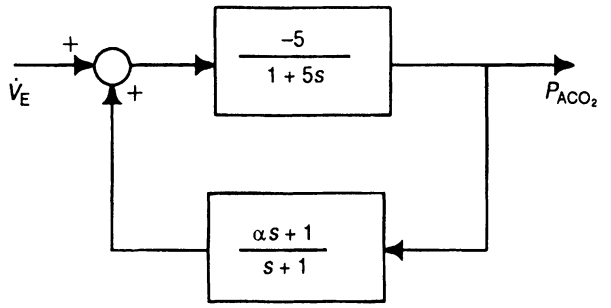

Figure P4.3 Simplified model of ventilatory control with intrapulmonary CO_2 receptor feedback.

element in the closed-loop system represents the gas exchange processes of the lungs, while the feedback element represents the dynamic characteristics of the intrapulmonary CO_2 receptors. The parameter α determines how rate-sensitive these receptors are. Determine the responses of this system to a large hyperventilatory sigh (which may be approximated by an impulse function) when: (a) $\alpha = 0$ (there is no rate sensitivity), (b) $\alpha = \frac{1}{2}$, and (c) $\alpha = 2$. (Note that the feedback element belongs to a class of systems known as lag-lead (when $\alpha < 1$) or lead-lag (when $\alpha > 1$) systems).

P4.5. Develop a SIMULINK program that simulates the linearized lung mechanics model shown in Figure 4.2b. Using the same parameter values as those given in Section 4.3, verify that you can obtain the impulse and step responses shown in Figures 4.4 and 4.5 for both open-loop and closed-loop circumstances.

P4.6. The SIMULINK program "`glucose.mdl`" is a dynamic version of the glucose regulation model discussed in Section 3.6. Determine the time-courses of the concentrations of glucose and insulin in response to the steady infusion of glucose at the rate of $80\,000\,\text{mg}\,\text{h}^{-1}$ for a period of 1 hour. The values of the other parameters are as given in Section 3.6. Compare these time-courses to the corresponding cases where the insulin production parameter, β, has been reduced to 20% of its nominal value.

P4.7. The degree of spasticity in patients with neuromuscular disorders can be quantified with the use of the "pendulum test." In this clinical procedure, the subject sits relaxed on a table with his lower leg initially supported by the medical examiner so that the knee joint is fully extended. The examiner abruptly releases the lower leg so that it swings freely until it finally comes to rest in the vertical position. The trajectory of the swing, as measured by the change in angle of knee flexion can reveal information about the neuromuscular stretch reflex. Modify the SIMULINK program "`nmreflex.mdl`" so that it can be used to simulate this test. Note that the major difference between the pendulum test and the procedure described in Section 4.6 is that, here, the externally applied moment does not remain constant but varies according to the angular displacement of the lower leg, since it

is a function of the weight of the lower leg and the moment arm between the center-of-gravity of the lower leg and the knee joint. Assume the same parameter values used in "`nmreflex.m`", except for the following: moment of inertia of the lower leg about the knee joint $= 0.25\,\text{kg}\,\text{m}^2$; length of lower leg $= 40\,\text{cm}$, weight of lower leg $= 5\,\text{kg}$. Determine how the trajectory of the lower leg would change with different values of stretch reflex gain β.